Effect of Overheating Temperature on Microstructure and Hardness of HP40 Nb Alloy: Analysis by ANOVA

Milica TIMOTIJEVIĆ [1], Mića ĐURĐEV [2], Olivera ERIĆ CEKIĆ [1, 3]*, Petar JANJATOVIĆ [4], Aleksandar DEVEČERSKI [5], Dragan RAJNOVIĆ [4]

[1] *Faculty of Mechanical and Civil Engineering in Kraljevo, University of Kragujevac, Dositejeva 19, 36000 Kraljevo, Serbia*
[2] *Department of Mechanical Engineering, Technical faculty "Mihajlo Pupin", University of Novi Sad, Djure Djakovica 6b, 23000 Zrenjanin, Serbia*
[3] *Innovation Center of Mechanical Engineering Faculty, University of Belgrade, Kraljice Marije 16, 11000 Belgrade, Serbia*
[4] *Faculty of Technical Science, University of Novi Sad, Trg Dosteja Obradovica 6, 21000 Novi Sad, Serbia*
[5] *Department of Materials, Vinča Institute of Nuclear Sciences, University of Belgrade, National Institute of the Republic of Serbia, Mike Petrovica Alasa 12-14, 11351 Vinca, Belgrade, Serbia*

http://doi.org/10.5755/j02.ms.37697

Received 20 September 2024; accepted 4 November 2024

In this study, the influence of short-term overheating on the microstructure and hardness of tube segments made of centrifugally cast austenitic alloy HP40 Nb that were exposed to high temperatures in a stream of hydrocarbons and water vapor, at low pressure for more than 100,000 hours has been studied. Samples were heated up to 1223, 1323, and 1423 K under air at different time intervals from 30 to 480 min, respectively. Microstructural investigation and chemical analysis of as-cast and heat-treated specimens were performed by scanning electron microscopy and energy dispersive spectroscopy. The results showed significant differences in microstructure and hardness after short-term overheating. The results obtained were analyzed using regression analysis and ANOVA methods. The highest hardness of 203.85 HV10 was obtained after overheating at 1223 K for 480 min. The test results were analyzed using regression analysis and ANOVA test. ANOVA test confirmed the results with a 71.82 % model representativeness for hardness. This paper provides insights into the effects of short-term overheating on the mechanical properties of HP40 Nb grade steel after long-term operating conditions at high temperatures, which may be significant for improving performance and predicting the remaining life of the tubes made of HP40 Nb.
Keywords: centrifugal cast tubes, steel, thermal treatments, hardness.

1. INTRODUCTION

Ethylene is produced by pyrolysis of a mixture of hydrocarbons and steam in reformer furnaces operating at high temperatures (1173 to 1373 K) and through which the gas mixture passes under a pressure of 2 – 4 MPa [1 – 3]. Centrifugally cast austenitic steel alloys of the H series, which are resistant to high temperatures, creep, and oxidation, are used to make tubes in furnaces. These tubes are key components in petrochemical plants. Although they are designed for long-term operation up to 100,000 hours in these aggressive working conditions, the actual service life can vary due to various damage mechanisms, including creep, carburization, oxidation, and frequent exposure to short-term overheating of the tubes [4 – 8]. Tube overheating occurs when there is a burner malfunction that heats the tubes in the ethylene production process or due to reduced flow through the tubes caused by coke deposition on the tube walls. Because of their exceptional creep strength, oxidation resistance, and superior mechanical properties for use in reformer furnaces, tubes made of HP40 Nb alloy are most used [9, 10]. In the as-cast state, the HP40 Nb alloy consists of primary NbC carbides and M_7C_3-type carbides rich in chromium, which are located along grain boundaries and between dendrites [11]. Under operating conditions, the secondary carbides are precipitated in the austenite matrix, while the primary carbides coarsen continuously. Upon exposure to high temperatures, M_7C_3-type carbides transform into $M_{23}C_6$ carbides, and NbC carbide tends to transform into the G-phase [12, 13]. The transformation of NbC carbide into the G-phase occurs in the temperature range of 973 to 1263 K, with the transformation temperature ranging from 1173 to 1223 K [13]. In addition to microstructural changes that occur due to short-term overheating, there are also changes in mechanical properties [14 – 16]. It is not uncommon for tubes to be damaged due to overheating, but also for tubes to undergo overheating without showing any visible damage.

ANOVA analysis has been used in many studies to determine the optimal process parameters for obtaining the best process results. Olufunmilayo et al. [17] used ANOVA analysis to define the differences between various thermal treatments on the microstructure and mechanical properties of the investigated alloy. Monica et al. [18] and Marwan [19] evaluated the importance of individual metal heat treatment parameters using ANOVA analysis to identify the key parameters influencing the tensile strength, impact strength, and alloy resistance. Von et al. [20] examined the influence of annealing length and cooling rate in intercritical

* Corresponding author: O. Eric Cekic
E-mail: *eric.o@mas.bg.ac.rs*

annealing and isothermal bainite treatment on the microstructure and mechanical properties of the investigated alloy using ANOVA analysis. Joseph and Alo [21] utilized ANOVA analysis to determine which of the heat treatments (annealing, normalization, and aging) provides the best values for hardness, fatigue, and the most optimal microstructure. Furthermore, ANOVA analysis has also been used to compare the quality of metal products from different manufacturers [22].

The research on how temperature overheating impacts the microstructure and hardness of HP40-Nb alloy provides crucial insights with practical applications in various industries, particularly those that use high-performance materials in extreme conditions. By understanding how overheating affects the alloy's properties, manufacturers can optimize production processes, enhance component performance, and prolong service life.

The present work aims to determine the effects of overheating on the microstructure and hardness of the HP40 Nb (Cr25Ni35Nb) furnace tube which had been in service in reforming plants for about 11.4 years. Furthermore, the regression analysis and ANOVA test were employed to examine the influence of the overheating treatment parameters on the hardness of the HP40 Nb grade steel after long-term operating conditions at high temperatures.

2. EXPERIMENTAL DETAILS

In this study, samples made from the austenitic steel alloy HP40 Nb, produced by centrifugal casting, were examined. All samples were cut from HP40 Nb radiant tubes which were used in an ethylene cracking unit. The exact locations where the sections were cut on the reformer columns in the respective plants are not precisely known. The tube segments, 350 mm in length, were cut from furnace regions that had been in use for 11.4 years. The operating conditions of the tubes were 1143 K (870 °C) under a maximum internal pressure of 250 kPa (2.5 bars). The chemical composition of the service reformer tube was analysed through standard analytical spectrometry method, using the Optical Energy Spectrometer (OES) type I Spark 8860, Thermo Scientific™, USA.

The specimens were heated up to 1223, 1323, and 1423 K at different time intervals of 30, 120, and 480 minutes in the electric furnace in an air atmosphere, and then each aged sample was cooled in air. The heating of the samples was performed in a chamber-type laboratory furnace with a PID temperature controller. The temperature was controlled by the thermocouple Pt-Pt13%Rh placed just above the sample.

Specimens for metallographic studies were prepared by standard metallographic preparation technique: grinding with SiC papers (from 180 to 2400), polishing with diamond suspensions (with 6, 3, 1, and ¼ μm particle size) and etching with a solution of 15 ml HCl, 10 ml Glycerol and 5 ml HNO_3.

The microstructure was examined using a scanning electron microscope JOEL JSM 6460 LV and the phases observed were analysed using an energy dispersive x-ray analyser system (EDS) INCA Oxford Instruments in conjunction with a SEM.

The Vickers hardness was assessed using a VEB HPO-250 apparatus with a 10 kgf load, and the mean value was derived from five random measurements, in compliance with the ISO 6507-1 standard.

The percentage of primary and secondary carbides in the microstructure after heat treatments was determined using the JMicroVision software.

3. RESULTS AND DISCUSSION

3.1. Microstructural results

The chemical composition of the investigated alloy consisted of: 0.45 %C, 0.97 %Mn, 1.36 %Si, 0.045 %P, 32.21 %Ni, 26.22 %Cr, 1.5 %Nb (mass %), and Fe balance.

The microstructure of the ex-service material depicted in Fig. 1 a, consists of the matrix, which is the austenite dendritic phase with a complex network of coarsened intergranular precipitates [16].

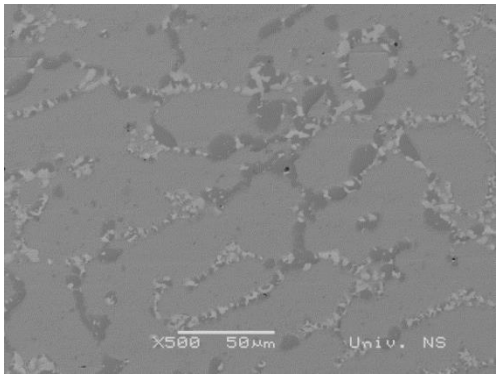

a

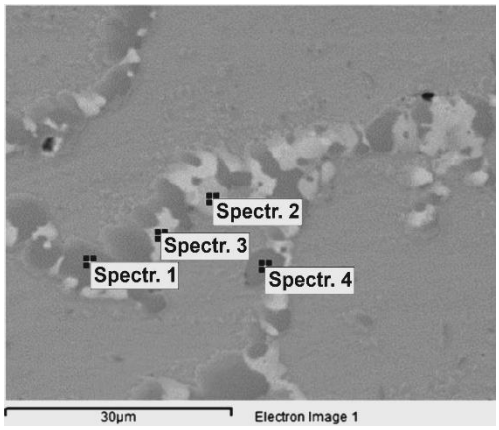

b

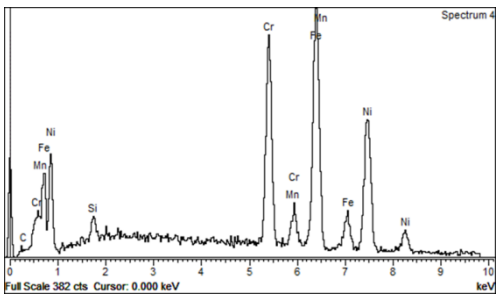

c

Fig. 1. SEM and EDS analysis of alloy in initial state: a – SEM micrograph of the sample taken from the inner surface; b – positions of EDS Spectrums in analysis; c – corresponding EDS spectrum 4

Analyzing the SEM micrograph (Fig. 1 b), two types of carbide precipitation can be categorized. Light grey carbides exhibit a more continuous and blockier morphology, while dark grey ones are predominantly situated within dendritic regions, as revealed by backscattered electrons. The microstructure confirmed by SEM-EDX studies (Table 1) consists of an austenitic matrix and a continuous network of primary eutectic carbides of two types: MC-type carbides rich in Nb (bright particles in Fig. 1 b, Spec. 2), M_7C_3-type carbides (M= Cr, Ni, Fe) rich in Cr (dark particles in Fig. 1 b, Spec. 1, 4) [23] and CrNiC phase (even brighter particles in Fig. 1 a and b, Spec. 3). Carbides present at inter-dendritic boundaries exhibit lamellar or skeletal forms.

Table 1. Chemical composition (mass. %) of participating phases in HP40 Nb alloy, according to Fig. 1 b

	C	Si	Cr	Mn	Fe	Ni	Nb
Spec. 1	30.3		58.8		6.5	4.4	
Spec. 2	20.6	10.8	30.8		4.6	21.0	12.3
Spec. 3	31.7	0.9	31.0		20.7	15.7	
Spec. 4	5.5	2.7	22.1	1.2	36.9	31.6	

In Fig. 2 a – c the microstructure of the samples after thermal treatment is shown. In Fig. 2 a, the microstructure of the tested tube sample (HP40 Nb) after overheating at 1223 K (950 °C) for 480 minutes is shown. It is observed that during this thermal treatment, secondary $Cr_{23}C_6$ carbide particles are formed in the microstructure, grouped near the dendrite boundaries as well as in the austenitic matrix in the form of inter-dendritic deposits (Fig. 2 a, marked in green).

Due to overheating at 1223 K for 480 minutes, the primary $M_7C_3/M_{23}C_6$ carbides transformed into coarse $M_{23}C_6$ carbides in the form of separated precipitates and significantly lost their lamellar shape. The NbC carbides are present as fine particles distributed in the austenitic matrix and along the dendrites. The overheating treatment of the sample at 1223 K for 480 minutes resulted in the precipitation of fine secondary carbide particles, which contributed to the increase in hardness. As the overheating temperature rises from 1223 to 1323 K, there is a gradual reduction in the number of secondary carbides present within the austenite matrix.

In Fig. 2 b, the microstructure of the same tube segment sample after overheating at 1323 K (1050 °C) for 480 minutes is shown. During this thermal treatment, the microstructure shows the decomposition of secondary $Cr_{23}C_6$ carbide particles, grouped along the dendrite boundaries (Fig. 2 b, marked in green). After overheating at 1323 K for 480 minutes, coarse primary $M_{23}C_6$ carbides in the form of separated chains are present, with a reduction in the amount of these carbides due to dissolution. Niobium carbides are in the form of fine particles grouped along the dendrites. At this overheating temperature, the microstructure contains a clean austenitic matrix without secondary chromium precipitates.

In Fig. 2 c, the microstructure after overheating at 1423 K (1150 °C) for 480 minutes is shown. During this heat treatment, the microstructure shows almost complete decomposition of secondary $Cr_{23}C_6$ carbide particles along the dendrite boundaries and between the dendrites. Along the dendrite boundaries, the deposition of remaining fine NbC carbide particles is observed.

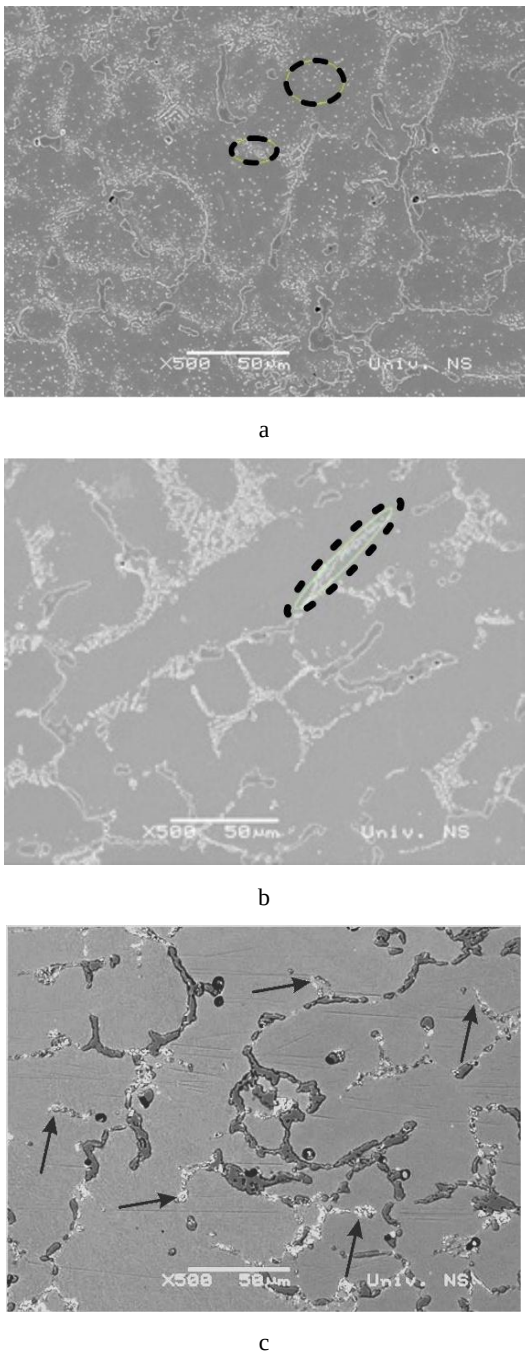

Fig. 2. SEM micrograph of the sample after thermal treatment after 480 minutes on: a – 1223 K; b – 1323 K; c – 1423 K

Coarse primary $M_{23}C_6$ carbides in the form of separated chains along the dendrite boundaries are present (Fig. 2 c). In some areas of the microstructure, carbide-free regions in the austenitic matrix are observed. At this overheating temperature, complete dissolution of the secondary precipitation, Nb-carbides disappear, i.e., they dissolve into the austenitic matrix.

Table 2 shows the alloy hardness test results, with an average hardness for each trial. The hardness test results of the specimens, post overheating treatment at temperatures of 1223, 1323, and 1423 K, indicate a higher hardness than that of the initially received specimen. Based on the measured hardness values presented in Table 2, it is observed that the hardness values are like those measured by other authors [15]. Additionally, from Table 2, it can be

concluded that the highest measured hardness values were observed in samples that were overheated for 480 minutes.

Table 2. The results of the hardness test

Heat temp., K	Hold time, min	Hardness HV10					Mean
		1	2	3	4	5	
1223	30	186	187	184	181	186	185
	120	186	184	187	188	185	186
	480	206	203	205	205	206	205
1323	30	182	180	183	176	180	181
	120	174	173	172	176	178	176
	480	191	189	191	191	190	190
1423	30	176	176	175	176	177	177
	120	176	178	178	184	173	178
	480	209	209	224	212	214	214

Also, it can be noted that the maximum hardness value is found in the sample heated at 1423 K for 480 minutes (1150 °C/480 min). After the thermal treatment of the sample at 1223 K for 480 minutes, the percentage content of primary and secondary carbides is 28.75 % primary carbides and 71.25 % secondary carbides. In the sample thermally treated at 1323 K for 480 minutes, the microstructure consists of 40.8 % primary carbides and 59.2 % secondary carbides. The microstructure of the sample thermally treated at 1423 K for 480 minutes consists of 66.75 % primary and 33.25 % secondary carbides. It can be observed that changes in the microstructure have a significant impact on the hardness variation of the alloy [24]. By examining the microstructure images of the samples after thermal treatments at 1223, 1323, and 1423 K for 480 minutes (Fig. 2 a – c), the measured hardness values after these thermal treatments, and the values of primary and secondary carbides in the samples treated at 1223, 1323, and 1423 K for 480 minutes, it can be concluded that the cause of the maximum hardness value in the sample treated at 1423 K for 480 minutes is the dissolution of chromium-rich carbides and the diffusion of carbon into the austenitic matrix.

The research analyzed the influence of overheating temperature and overheating time on the hardness of ethylene furnace tube materials made of HP40 1.5 % Nb. The results were collected after a series of measurements where the temperature and overheating time were varied, with certain measurements replicated to obtain more reliable results.

The transformation of carbides in HP40 alloys during heating cycles has been extensively studied. In as-cast conditions, the microstructure consists of an austenitic matrix with primary carbides, including M_7C_3, $M_{23}C_6$, and MC types [16, 28]. During aging, several transformations occur: M_7C_3 transforms to $M_{23}C_6$, secondary $M_{23}C_6$ carbides precipitate, and NbC transforms to G-phase ($Ni_{16}Nb_6Si_7$) [16, 20, 28].

The transformation of NbC carbides in HP40-Nb alloys during high-temperature aging has been extensively studied. NbC carbides transform into G-phase (Ni16Nb6Si7) silicide, starting at the carbide-matrix interface and progressing inward [27, 28]. This transformation involves a complex microstructure with an untransformed NbC core, an intermediate G-phase layer containing nanometric TiC precipitates, and an outer shell of alternating $Cr_{23}C_6$ and G-phase [27]. Experimental techniques such as SEM, TEM, XRD, and EBSD coupled with EDS have been employed to study these transformations [27].

3.2. Statistical analysis using the ANOVA test

Statistical analysis is performed using Minitab 20 statistical software. Analysis of variance (ANOVA) and regression analysis are evaluated using F-tests with a 95 % confidence interval, corresponding to a level of significance $p = 0.05$. Based on the experimental findings, ANOVA analysis, regression analysis, and subsequent parameter optimization were conducted to determine the factors affecting tube hardness.

The results of the ANOVA analysis presented in Table 3 confirm the statistical significance of the overall regression model with a high F-value of 12.75, exceeding the critical F-cr value, and a low P-value of 0.002 that is below the level of significance of 0.05. Specifically, overheating emerges as a statistically significant factor, while on the other hand, the overheating temperature does not show a significant influence on tube hardness. The high lack-of-fit error value indicates a problem of model adaptability, as the variations in the obtained results are not fully described.

The coefficients of the ANOVA regression equation are given in Table 4.

Table 3. Analysis of variance summary table for hardness HV10

Source	DOF	Adj SS	Adj MS	F-value	P-value	Percentage, %
Regression	2	1267.93	633.97	12.75	0.002	71.82
Overheating temperature	1	28.90	28.90	0.58	0,463	1.64
Overheating time	1	1116.54	1116.54	22.45	0.001	63.25
Error	10	497.30	49.73			28.17
Lack-of-fit	6	478.79	79.80	17.24	0.008	27.12
Pure rrror	4	18.52	4.63			1.05
Total	12	1765.24				100
*DOF – degrees of freedom, Adj SS – adjusted sum of squares, Adj MS – adjusted mean squares						

Table 4. The regression coefficients obtained in Minitab

Terms	Coef	SE Coef	T-Value	P-Value	VIF
Constant	195.5	26.8	7.30	0.000	
Overheating temperature	-0.0185	0.0243	-0.76	0.463	1.04
Overheating time	0.0540	0.0114	4.74	0.001	1.04
*Coef – regression coeficients, SE Coef – standard error of coefficents, VIF – variance inflation factor					

The regression analysis yielded a regression equation for the multiple linear model dependence on input factors: tube overheating temperature and time:

$$HV10 = 195.5 - 0.0185 \times \text{Overheating temperature} + 0.0540 \times \text{Overheating time}. \quad (1)$$

This model explained 71.82 % of the variability in measurements, indicating a relatively high model efficiency in explaining the change in material hardness due to changes in input factors. The high p value of 0.463 for overheating temperature indicates that it is less significant on the

dependent variable, HV10. On the other hand, a low p value for overheating time has a more reliable influence on hardness HV10.

Optimization of the overheating parameters of ethylene furnace tubes was performed using the Matlab software package. For the objective function, an experimentally obtained regression equation for hardness HV10 was selected. Regarding the overheating parameters, temperature and time were defined by their upper and lower bounds (Upper and Lower Bounds):

1. Lower and upper bounds for temperature: (950, 1150);
2. Lower and upper bounds for time: (30, 480).

To determine the optimal results, specifically to identify the maximum – critical HV10 hardness value, optimization was carried out using three different metaheuristic algorithms: Particle Swarm Optimization (PSO), Honey Badger Algorithm (HBA), and Grey Wolf Optimizer (GWO). Each algorithm was run 20 times (20 runs) in 100 iterations. The population size was 20.

Table 5 shows the optimization results. As can be seen, all algorithms achieved identical solutions for HV10 hardness, with a value of 203.845. The optimal parameters, temperature and time of tube overheating, obtained were 1223 K (950 °C) and 480 minutes. Given the frequency of this result, the algorithms achieved average results without standard deviation. On each run of the algorithm, the results are identical. Based on the presented data, we can conclude that metaheuristic algorithms prove to be very efficient tools for solving these types of optimization problems.

Table 5. Optimization results of overheating parameters using metaheuristic algorithms

Performance measures	PSO	HBA	GWO
Best fitness	203.845	203.845	203.845
Mean fitness	203.845	203.845	203.845
Std. Deviation	0	0	0

4. CONCLUSIONS

Based on the results obtained from the experiment, the following conclusion can be drawn:

1. The microstructure of the ex-service material consists of the austenite dendritic phase matrix with a sophisticated network of coarsened intergranular precipitates.
2. Due to overheating at 1223 K for 480 minutes, the primary $M_7C_3/M_{23}C_6$ carbides transformed into coarse $M_{23}C_6$ carbides in the form of separated precipitates and significantly lost their lamellar shape.
3. The overheating treatment of the sample at 1223 K for 480 minutes resulted in the precipitation of fine secondary carbide particles, which contributed to the increase in hardness.
4. As the overheating temperature rises from 1223 to 1323 K, there is a gradual reduction in the number of secondary carbides present within the austenite matrix.
5. During overheating treatment at 1423 K for 480 min, the microstructure shows almost complete decomposition of secondary $Cr_{23}C_6$ carbide particles along the dendrite boundaries and between the dendrites. At this overheating temperature, complete dissolution of the secondary precipitation, Nb-carbides disappear, i.e., they dissolve into the austenitic matrix.
6. The ANOVA revealed that the hardness level of HP40 Nb alloy is influenced by two factors: overheating temperature and overheating time.
7. The results of the ANOVA analysis confirm the statistical significance of the overall regression model with a high F-value of 12.75, exceeding the critical F-cr value, and a low P-value of 0.002. Furthermore, the ANOVA test confirmed the results with a 71.82 model representativeness for hardness.
8. The optimized conditions achieved were an overheating temperature of 1423 K and an overheating period of 480 min.

Acknowledgments

This work was supported by the Ministry of Science, Technological Development and Innovation of the Republic of Serbia, Contract No.: 451-03-65/2024-03/200108, Faculty of Mechanical and Civil Engineering in Kraljevo, University of Kragujevac; 451-03-66/2024-03/200213, Innovation Centre of the Faculty of Mechanical Engineering, Belgrade, University of Belgrade; 451-03-65/2024-03/200156 and No. 01-3394/1 by Faculty of Technical Science, University of Novi Sad, Grant no. 451-03-66/2024-03/200017 Department of Materials, Vinča Institute of Nuclear Sciences, University of Belgrade, National Institute of the Republic of Serbia.

REFERENCES

1. **Voicu, R., Lacaze, J., Andrieu, E., Poquillon, D., Furtado, J.** Creep and Tensile Behaviour of Austenitic Fe-Cr-Ni Stainless Steels *Materials Science and Engineering A* 501 – 511 2009: pp. 185 – 189. https://doi.org/10.1016/j.msea.2008.04.098
2. **Brear, J., Chuech, J., Humphrey, D., Zanjani, M.** Life Assessment of Steam Reformer Radiant Catalyst Tubes – the Use of Damage Front Propagation Methods *International Journal of Pressure Vessels and Piping* 78 (11 – 12) 2001: pp. 985 – 994. https://doi.org/10.1016/S0308-0161(01)00113-2
3. **Wang, F., Northwood, D.** The Effect of Carbon Content on The Microstructure of an Experimental Heat-Resistant Steel *Materials Characterization* 31 (1) 1993: pp. 3 – 10. https://doi.org/10.1016/1044-5803(93)90039-X
4. **Hamid, Ul., Tawancy, HM, Mohamed, AI, Abbas, NM.** Failure Analysis of Furnace Radiant Tubes Exposed to Excessive Temperature *Engineering Failure Analysis* 13 (6) 2006: pp. 1005 – 1021. https://doi.org/10.1016/j.engfailanal.2005.04.003
5. **Guan, K, Xu, H, Wang, Z.** Analysis of failed ethylene cracking tubes *Engineering Failure Analysis* 12 2005: pp. 420 – 431. https://doi.org/10.1016/j.engfailanal.2004.03.012
6. **Ferreira, H.** Investigation of an Unusual Reformer Tube Failure. IMTOF 97, 1997.
7. **De Silveira, T.L., Le May, I.** Reformer Furnaces: Materials, Damage, Mechanisms and Assessment *The Arabian Journal of Scientific Engineering* 31 (2) 2006: pp. 99 – 119.
8. **Swaminathan, J., Guguloth, K., Gunjan, M., Roy, P., Ghosh, R.** Failure Analysis and Remaining Life Assessment

of Service Exposed Primary Reformer Heater Tubes *Engineering Failure Analysis* 15 2005: pp. 311 – 331. https://doi.org/10.1016/j.engfailanal.2007.02.004

9. **Allahkaram, S.R., Borjali, S., Khosravi, H.** Investigation of Weldability and Property Changes of High Pressure Heat-Resistant Cast Stainless Steel Tubes Used in Pyrolysis Furnaces after a Five-Year Service *Materials Design* 33 2012: pp. 476 – 484. https://doi.org/10.1016/j.matdes.2011.04.052
10. **Shen, L.M., Gong, J.M., Jiang, Y., Geng, L.Y.** Effects of Aging Treatment on Microstructure and Mechanical Properties of Cr25Ni35Nb and Cr35Ni45Nb Furnace Tube Steel *Acta Metallurgica Sinica* 24 (3) 2011: pp. 235 – 242. https://www.amse.org.cn/EN/Y2011/V24/I3/235
11. **Ma, Y.W., Yang, G., Yoon, K.B., Le, T.G.** Microstructure Evaluation during Short Term Creep of $Cr_{35}Ni_{45}Nb$ Cast Alloy Reformer Tube *Metals and Materials International* 27 2021: pp. 5165 – 5172. https://doi.org/10.1007/s12540-020-00862-y
12. **Nascimento, M., Gallo, F., Queiroz, F., Mendes, M., Eckstein, C., Nogueira, L., May, I., Pereira, G., de Almeida, L.** Effect of Short-Time Overheating in the Morphology of Primary Carbides Network in Nb and NbTi-Modified HP Stainless Steels Steam Reforming Tubes *Journal of Materials Research and Technology* 22 2023: pp. 382 – 392. https://doi.org/10.1016/j.jmrt.2022.11.130
13. **Fuyang, C., Chen, J., Shao, B., Zhou, Y., Gong, J., Guo, X., Jiang, Y.** Effect of Microstructural Evolution in Thermal Exposure on Mechanical Properties of HP40Nb alloy *Internacional Journal of Pressure Vessels and Piping* 192 2021: pp 1 – 11. https://doi.org/10.1016/j.ijpvp.2021.104391
14. **Fuyang, C., Zhu, R., Zhang, P., Guo, X.** Feasibility Assessment of Local Repairment for Reformer Furnace Tubes in Service Exposure *International Journal of Pressure Vessels and Piping* 179 2020: pp. 1 – 11. https://doi.org/10.1016/j.ijpvp.2019.104032
15. **Ray, A., Kumar, S., Krishna, G., Gunjan, M., Goswami, B., Bose, S.** Microstructural Studies and Remnant Life Assessment of Eleven Years Service Exposed Reformer Tube *Material Science and Engineering* A 529 2011: pp. 102 – 112. https://doi.org/10.1016/j.msea.2011.09.003
16. **Timotijević, M., Erić Cekić, O., Rajnović, D., Dojčinović, M., Janjatović, P.** Microstructure Evolution and Mechanical Properties Degradation of HPNb Alloy after an Eleven-Year Service *Structural Integrity and Life* 22 (3) 2022: pp. 299 – 304.
17. **Olufunmilayo, J., Olakunle, J., Oluwafemi, L.** Effect of Heat Treatment on Microstructure and Mechanical Properties of SAE 1025 Steel: Analysis by One-Way ANOVA *Journal of Materials and Environmental Science* 6 (1) 2015: pp. 101 – 106.
18. **Monica, V., Lakshmikanth, G., Lathicashree, S., Senthilkumar, N., Muniappan, A., Deepanraj, B.** An Experimental Analysis and Optimization of Heat Treatment Parameters of Aluminium 6061 Alloy for Improved Mechanical Properties *International Journal of Mechanical and Production Engineering Research and Development* 9 2019: pp. 46 – 59.
19. **Marwan, A., Ali Saad, M., Hamed, J., Al Hifadhi, M.** Effects of Heat Treatment on the Corrosion and Mechanical Properties of Stainless Steel 316L as Used in Biomedical Applications *IOP Conference Science and Engineering* 1067 (1) 2021: pp. 1 – 18. https://doi.org/10.1088/1757-899X/1067/1/012142
20. **Von, H., Van, Ch., Ngoc, T., Manh, T.** Influence of Heat Treatment on Microstructure and Mechanical Properties of a CMnSi TRIP Steel Using Design of Experiment *Materials Today Proceedings* 5 (1) 2018: pp. 24664 – 24674. https://doi.org/10.1016/j.matpr.2018.10.264
21. **Joseph, O., Alo, F.** An Assessment of the Microstructure and Mechanical Properties of 0.26 % Low Carbon Steel under Different Cooling Media: Analysis by One-Way ANOVA *Industrial Engineering Letters* 4 (7) 2014: pp. 39 – 46.
22. **Alo, F., Atanda, P., Daniyan, A., Abodunrin, O., Oluwasegun, K.** An Assessment of Imported and Local Constructional Steel in Nigeria: Analysis by One-Way ANOVA *International Journal of Materials Engineering* 7 (3) 2017: pp. 45 – 51. https://doi: 10.5923/j.ijme.20170703.01
23. **Ghatak, A., Robi, P.** Effect of Temperature on The Microstructure and Hardness of Service Exposed 25Cr35NiNb Reformer *Tubes Transactions of the Indian Institute of Metals* 2015: pp. 823 – 827. https://doi.org/10.1007/s12666-015-0552-6
24. **Ghatak, A., Robi, P.** Effect of Microstructure with Hardness on Heat Treatment of HP40Nb Microalloyed Reformer Tube *5th International & 26th All India Manufacturing Technology, Design and Research Conference* 2014: pp. 471 – 474. https://www.researchgate.net/publication/275889261
25. **Picasso, A., Lanz, C., Sosa, M.** Microstructure Evolution of a Nickel-Base Alloy Resistant to High Temperature during Aging *Journal of Minerals and Materials Characterization and Engineering* 4 2016: pp.48 – 61. https://doi:10.4236/jmmce.2016.41006
26. **Lanz, C., Brizuela, G., Juan, A., Simonetti, S.** Microstructural Evolution of a Modified HP Alloy: Experimental and Complementary Computational Study *Journal of Advance Physics* 13 (9) 2017: pp. 5141 – 5145. https://doi.org/10.24297/jap.v13i9.6415
27. **Vaché, N., Steyer, P., Duret-Thual, C., Perez, M., Douillard, T., Rauch, E., Véron, M., Renou, G., Dupoiron, F., Augustin, C., Cazottes, S.** Microstructural Study of the NbC to G-phase Transformation in HP-Nb Alloys *Materialia* 9 2020: pp. 100593. https://doi.org/10.1016/j.mtla.2020.100593
28. **Lissarrague, M.H.S., Lanz, C.A.** NbC Transformation during Aging in HP40-Nb Heat Resistant Alloy *Acta Metallurgica Slovaca* 28 (3) 2022: pp. 147 – 150. https://doi.org/10.36547/ams.28.3.1562